Influence of breakup on elastic and α-production channels in the ^{6}Li+^{116}Sn reaction *

D. Patel[1;1)] S. Mukherjee[2;2)] N. Deshmukh[3] J. Lubian[4] Jian-Song Wang(王建松)[1]
T. Correa[5] B. K. Nayak[6] Yan-Yun Yang(杨彦云)[1] Wei-Hu Ma(马维虎)[1]
D. C. Biswas[6] Y. K. Gupta[6] S. Santra[6] E. T. Mirgule[6]
L. S. Danu[6] N. L. Singh[2] A. Saxena[6]

[1] CAS Key Laboratory of High Precision Nuclear Spectroscopy and Center for Nuclear Matter Science, Institute of Modern Physics, Chinese Academy of Sciences, Lanzhou 730000, China
[2] Department of Physics, Faculty of Science, The M. S. University of Baroda, Vadodara-390002, India
[3] INFN Laboratori Nazionali del Sud, Catania, Italy
[4] Instituto de Fısica, Universidade Federal Fluminense, Av. Litoranea s/n, Gragoatá, Niteroi, R.J., 24210-340, Brazil
[5] Instituto de Aplicação Fernando Rodrigues da Silveira, Universidade do Estado do Rio de Janeiro, R. Santa Alexandrina 288, Rio Comprido, Rio de Janeiro, RJ, 20261-232, Brazil
[6] Nuclear Physics Division, Bhabha Atomic Research Centre, Mumbai-400085, India

Abstract: The effects of breakup reactions on elastic and α-production channels for the ^{6}Li+^{116}Sn system have been investigated at energies below and near the Coulomb barrier. The angular distributions of α-particle production differential cross sections have been obtained at several projectile energies between 22 and 40 MeV. The measured breakup α-particle differential cross sections and elastic scattering angular distributions have been compared with the predictions of continuum-discretized coupled channels (CDCC) calculations. The influence of breakup coupling has also been investigated by extracting dynamic polarization potentials (DPP) from the CDCC calculations. From the predictions of CDCC calculations the relative importance of the nuclear, Coulomb, and total breakup contributions have also been investigated. The nuclear breakup couplings are observed to play an important role in comparison to the Coulomb breakup for the direct breakup mechanisms associated in the reaction of ^{6}Li projectile with ^{116}Sn target nuclei. The influence of strong nuclear breakup coupling exhibits suppression in the Coulomb-nuclear interference peak. The direct breakup cross sections from the CDCC calculations under-predict the measured α-particle differential cross sections at all energies. This suggests that the measured α particles may also have contributions from other possible breakup reaction channels.

Keywords: elastic scattering, α-production channels, breakup coupling effects, dynamic polarization potentials

PACS: 25.70.Bc, 25.70.Mn, 24.10.Eq **DOI:** 10.1088/1674-1137/41/10/104001

1 Introduction

In the last few decades, reaction studies with loosely bound nuclei such as ^{6,7}Li and ^{9}Be have drawn considerable interest due to their structural similarity to unstable weakly bound nuclei. Stable weakly bound projectiles with low breakup thresholds are well-suited candidates for breakup reaction studies due to their easy access and the more intense beams that can be produced with them. In the past few years, several theoretical as well as experimental attempts have been made towards an understanding of the way the structures of colliding nuclei influence the course of the different reaction channels. More recently, the influence of projectile breakup on elastic scattering and fusion cross section has been extensively investigated in reactions with stable weakly bound and also for exotic nuclei [1–9]. Elastic scattering studies are the easiest and most widely used alternative for exploring breakup coupling effects on different reaction channels. The energy dependence of potential parameters extracted from the elastic scattering can unravel the breakup mechanisms at energies near the Coulomb barrier [10, 11]. In reactions with weakly bound nuclei, it has been shown that the breakup chan-

Received 3 May 2017

∗ One of the authors (SM) would like to thank DAE-BRNS for financial assistance through a major research project. This work is supported by National Natural Science Foundation of China (U1432247, 11575256, U1632138, 11605253) and China Postdoctoral Science Foundation (2016M602906)

1) E-mail: kherdipika2006@gmail.com
2) E-mail: sk.mukherjee-phy@msubaroda.ac.in

nel does not vanish in the vicinity of the Coulomb barrier; rather, it can have some magnitude owing to the coupling of the breakup channel to the continuum producing a repulsive polarization potential. This is in contradiction with the observation made in the case of tightly bound projectile nuclei. The above observations can be further explored by means of the continuum discretized coupled channels (CDCC) formalism. This has been proved an effective method to take into account the coupling effects of breakup on the elastic scattering and fusion process. The dynamic polarization potential (DPP) that includes coupling effects can provide a qualitative idea of major couplings that have a significant effect on the reaction dynamics [12–16].

Reaction studies with weakly bound nuclei of cluster structure have found substantially large cross sections for breakup-α particles compared to the production of the complementary fragment [17–21]. This suggests a more complex nature for breakup processes and thus indicates the possibilities of various other reaction channels that contribute to the production of breakup-α particles. In Ref. [22], inclusive cross sections of the α particle yield have been measured for the ^{6}Li+^{159}Tb system, and found to be orders of magnitude larger than the calculated cross sections of ^{6}Li breaking into α and d fragments, thus indicating contributions from other processes. Recently, for the ^{6}Li+^{112}Sn system [23], direct breakup (α+d) and sequential breakup (1n-stripping and 1d-pickup) have been observed as the major projectile-breakup channels. For the reaction ^{7}Li+^{159}Tb, about half of the α and t yield was observed to be from the incomplete fusion (ICF) process, which is basically the breakup-fusion process [20]. The α particles coming from the transfer-induced breakup were also observed in the reaction of ^{7}Li with a ^{65}Cu target [24]. In Ref. [25], coincidence measurements of breakup fragments were carried out for the ^{7}Li+^{144}Sm and ^{6,7}Li+^{207,208}Pb, ^{209}Bi reactions at sub-barrier energies. It has been observed that the breakup is predominantly triggered by transfer leading to ^{5}Li(α+p) by n stripping for the projectile ^{6}Li.

Though the large production of breakup-α yield is common for various weakly bound projectile-target combinations, many factors affect the observation of large breakup-α. For example, the bombarding energies, reaction Q-values and also the projectile-target masses involved in the reaction studies are equally important to consider to understand the breakup mechanisms with a ^{6}Li projectile. Thus, the breakup-α angular distribution measurements in singles mode near and below the Coulomb barrier energies may also help in understanding the breakup reactions involving weakly bound projectiles with different breakup thresholds. Moreover, in a systematic study [26], it has been shown that the breakup-α cross sections display a simple $1/E_n$ (where E_n is the lowest neutron emission threshold for the projectile) power law behavior, at above-barrier energies. On the other hand, at sub-barrier energies it appears to be dependent on the details of nuclear structure of the interacting nuclei [26]. In our earlier work [27] with the present system, we have done optical model calculations for measured elastic scattering angular distributions and extracted optical potential parameters.

In the present work, an attempt has been made to explore the breakup coupling effects on elastic scattering and the measured breakup-α channel. We have measured breakup-α angular distributions near and below the Coulomb barrier energy for the ^{6}Li+^{116}Sn system. The dynamic polarization potentials ($V_{\rm pol}$, $W_{\rm pol}$) generated from breakup coupling have also been studied in this energy regime.

This paper is organized as follows. Section 2 describes the experimental details of the measurement of breakup-α angular distributions at energies near and below the Coulomb barrier. In Section 3, we present a brief description of the CDCC calculations. Also, the results of the calculations for ^{6}Li scattering from a ^{116}Sn target are described. Section 4 presents the angular distributions of α-particle production differential cross sections along with the results of direct breakup from the CDCC calculations. Finally, in Section 5, we present a summary and the conclusions of our work.

2 Experimental details

The measured α particles were detected and identified using the same setup from which the elastic scattering angular distribution measurement was carried out. The experiment was performed at the Bhabha Atomic Research Center-Tata Institute of Fundamental Research (BARC-TIFR) Pelletron, Mumbai, India. The typical beam current ranged between 2.5 and 30 nA. A self-supported enriched ^{116}Sn target of thickness 450 μg/cm^2 was used. The beam energies were corrected for the half target thickness in the analysis process, and amounted to a maximum of 92 keV for 20 MeV and a minimum of 63 keV for 35 MeV for the ^{6}Li+^{116}Sn system. The elastically scattered ^{6}Li ions and α particles were detected by three solid-state silicon surface barrier detectors in $\Delta E-E$ telescopic arrangements. The angular distributions were measured in steps of 2.5°–5° at angles from 20° to 173° at lower energies and from 20° to 105° for higher energies. Figure 1 shows a typical bi-parametric $\triangle$E-E spectrum for the ^{6}Li+^{116}Sn system at $E_{\rm lab}$=35 MeV and $\theta = 35°$. Good separation is achieved for both charge and mass in this experimental setup. Further experimental details are given in Ref. [27].

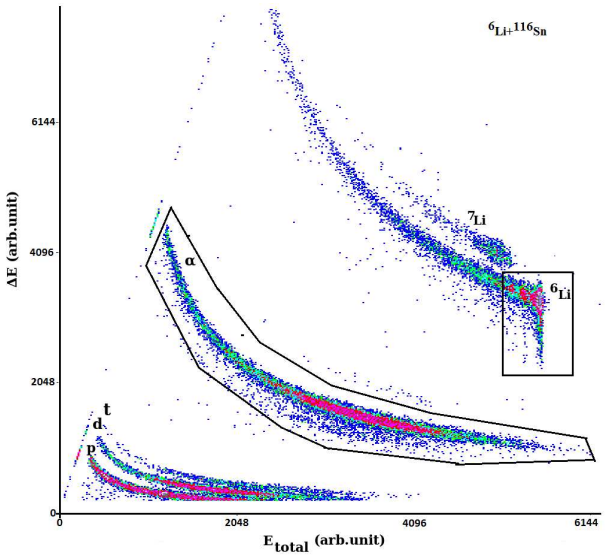

Fig. 1. A typical bi-parametric ΔE+E spectrum for the ^{6}Li+^{116}Sn system at $E_{\rm lab}$= 35 MeV and θ = 35°

3 Continuum discretized coupled channels calculations and results

The continuum discretized coupled channel (CDCC) method [28, 29] has been proved to be the best theoretical tool to study the couplings of continuum states among themselves and with bound states. Scattering states are grouped to form wave packets, or bins, belonging to the Hilbert space. Non-infinite matrix elements are obtained folding the interaction potential between the bin states. We can then couple the continuum states in the same way we proceed with inelastic excitations, but with a larger model space. The configuration space considered should in principle be infinite, but in practice it has to be truncated with the hope that the more important states are retained in the coupling scheme. Due to all these particularities, to obtain a numerical solution by means of the CDCC method is not easy and the convergence must be checked exhaustively.

To account for the breakup of the ^{6}Li in the ^{6}Li+^{116}Sn reaction we used a similar model space to that reported in Refs. [30, 31]. The ^{6}Li nucleus is treated as an α core plus one deuteron with a separation energy of 1.47 MeV. The states of the projectile are in the continuum and are approximated by a set of square-integrable bin wave functions. The bins are linear combinations of α+d scattering states, with centroids ε_i at α-d relative energies in the range $1.48< \varepsilon_i<\varepsilon_{\rm max}$. We used $\varepsilon_{\rm max}$=7 MeV. In this work we performed additional tests of convergence with the R-matrix method.

The CDCC calculations have been performed using Fresco code [32]. The transition matrix-elements were calculated for $r_{\rm bin}\leqslant$50 fm. This was enough to guarantee orthogonality between the bin states. The projectile-target distance in the solution of the coupled channels system was integrated numerically up to $R_{\rm max}$=500 fm and relative angular momenta up to 1000$\hbar$ were considered. The Woods-Saxon potentials used to generate the projectile's ground state $J^{\pi}=1^{+}$ and unbound resonant states 3^{+}, 2^{+} and 1^{+} were the same as those used in Refs. [30, 31]. We have used a double folding Sao Paulo Potential (SPP) [33] for the real part of the α, d+^{116}Sn optical potential. The imaginary part of the potential was taken as $W=0.78\times V_{\rm SPP}$, describing the elastic scattering of each cluster of the projectile. This is similar to the Akyüz-Winther potential at near-barrier energies. A similar procedure has been successfully used for many reaction studies [34].

For the lower energies the R-matrix method was used for the calculations of the cross section because at these energies the residual energy of the fragments is not high enough to access the higher energy bins, which remain as virtual states. With the S-Matrix these states are not well resolved, giving unphysical results (cross section not equal to zero). For the higher energies these states become accessible, and calculations by means of the S-matrix method are enough.

To investigate the effects of the pure Coulomb and pure nuclear couplings in the breakup reactions, we have performed independent calculations considering only the Coulomb and/or the nuclear part of the coupling interaction. In this technique we neglect all off-diagonal matrix elements of either the nuclear or the Coulomb part of the potential. More details can be found in Ref. [34].

The results of the elastic cross section from the above CDCC calculations are compared with the present experimental data in Fig. 2. The calculations reproduce the elastic scattering data reasonably well over the entire energy range of our measurement. The effects of the Coulomb couplings are clearly seen at forward angles while the nuclear couplings come into play at backward angles. The transition angle from the Coulomb to the nuclear coupling increases as the bombarding energy decreases. A large Coulomb+nuclear breakup coupling effect can be seen on the elastic scattering cross section at energies above the Coulomb barrier and it reduces gradually as the energy approaches the Coulomb barrier. In Fig. 3, aiming to emphasize the Coulomb-nuclear interference peak region, the elastic scattering angular distributions are shown with a linear scale for two different incident energies (30 MeV and 20 MeV) above and below the Coulomb barrier energy. The details of the different curves are same as described before in the text. From Fig. 3, one can clearly see that at both incident energies the nuclear coupling is strong and there is suppression in the Coulomb-nuclear interference peak. Similar observations have also been made in the reaction of ^{11}Be with

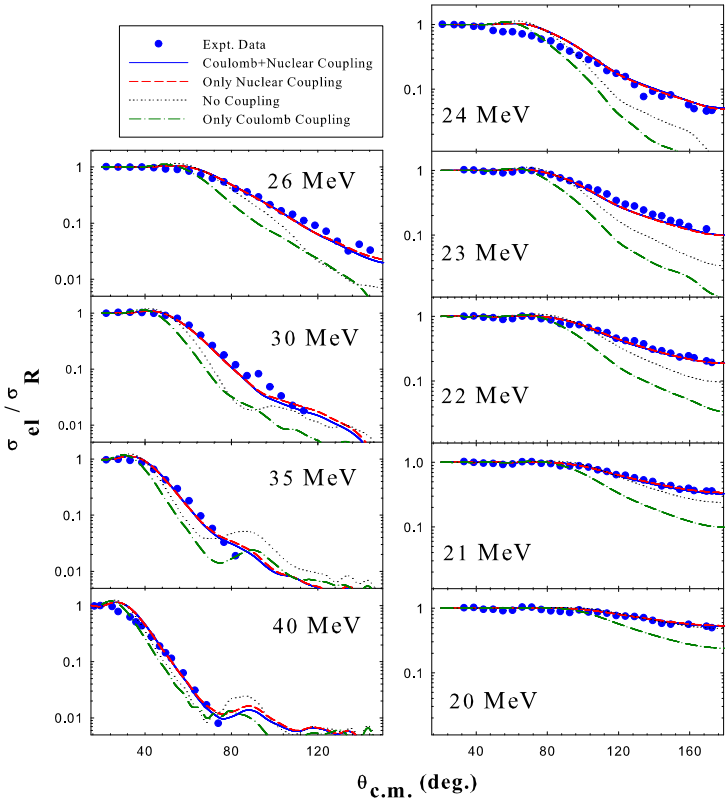

Fig. 2. (color online) Experimental elastic scattering cross sections normalized to the Rutherford cross sections as a function of $\theta_{\rm c.m.}$ for the ^{6}Li+^{116}Sn system. The results of the CDCC calculation for direct breakup of ^{6}Li into α+d with only Coulomb, only nuclear and Coulomb+nuclear breakup couplings are shown by dot-dashed, dashed and continuous curves respectively. The results without any coupling are shown by the dotted curves.

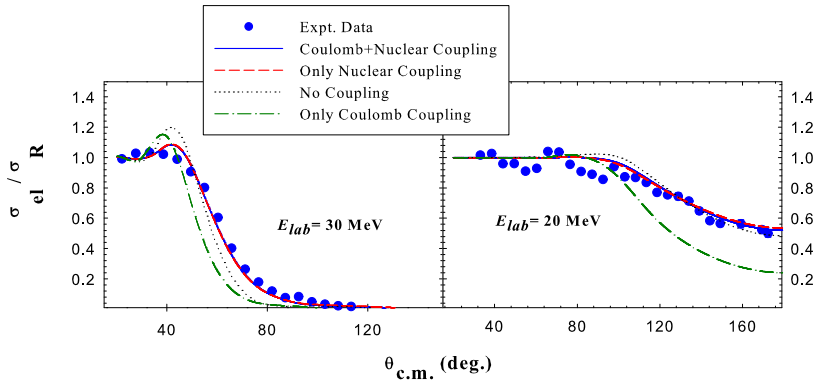

Fig. 3. (color online) Experimental elastic scattering cross sections normalized to the Rutherford cross sections as a function of $\theta_{\rm c.m.}$ for the ^{6}Li+^{116}Sn system (symbols), (a) at $E_{\rm lab}$= 30 MeV and (b) $E_{\rm lab}$=20 MeV. The results of the CDCC calculation for direct breakup of ^{6}Li into α+d with only Coulomb, only nuclear, and Coulomb+nuclear breakup couplings are shown by dot-dashed, dashed and continuous curves respectively. The results without any coupling are shown by the dotted curves.

a ^{64}Zn target, where it was observed that the unusual behavior of ^{11}Be is mainly due to the nuclear coupling to the continuum in ^{11}Be nuclei [35, 36]. Moreover, from the breakup cross sections given in Table 1, the nuclear breakup cross sections ($\sigma_{\rm bu}^{\rm nucl.}$) are systematically larger than the Coulomb breakup at all energies and at the lowest incident energy it is larger than the total breakup cross section ($\sigma_{\rm bu}^{\rm tot}$). The total breakup cross sections

($\sigma_{\rm bu}^{\rm tot}$) cannot be obtained by simply adding the nuclear and the Coulomb breakup cross sections. Also, the ratio of $(\sigma_{\rm bu}^{\rm tot}-\sigma_{\rm bu}^{\rm nucl.})/\sigma_{\rm bu}^{\rm coul.}$ is found to be less than one at all energies from above to below the barrier energy. This clearly shows destructive Coulomb-nuclear interference in the breakup process. In Ref. [37], a similar observation was made for the ^{6}Li+^{208}Pb system, which showed the dominance of Coulomb breakup.

Table 1. The direct breakup (α+d) cross sections with nuclear+Coulomb breakup coupling ($\sigma_{\rm bu}^{\rm tot}$), with only nuclear breakup coupling ($\sigma_{\rm bu}^{\rm nucl.}$), and with only Coulomb breakup coupling ($\sigma_{\rm bu}^{\rm coul.}$), from the CDCC calculations for the ^{6}Li+^{116}Sn system. The cross sections are given in mb.

$E_{\rm c.m.}$/MeV	$\sigma_{\rm bu}^{\rm tot}$	$\sigma_{\rm bu}^{\rm nucl.}$	$\sigma_{\rm bu}^{\rm coul.}$	$\frac{\sigma_{\rm bu}^{\rm tot}-\sigma_{\rm bu}^{\rm nucl.}}{\sigma_{\rm bu}^{\rm coul.}}$
19.02	11.7	13.2	9.0	-0.16
19.97	18.3	17	11.20	0.12
20.92	28.1	25.1	13.33	0.23
21.87	37.1	33.3	15.36	0.25
22.82	44.2	40	17.31	0.24
24.72	55.3	52	21.20	0.16
28.52	85.3	79	27.22	0.23
33.28	109	103	33.24	0.18
38.03	127	118	37.83	0.24

In a scattering study using weakly bound nuclei, the observation of the "breakup threshold anomaly (BTA)" [27] is mainly due to the strong coupling to the breakup channels, indicating an increase in imaginary potential strength with the corresponding decrease in real potential strength. The behavior of the energy dependence of the interacting potential obtained by the scattering of ^{6,7}Li on different target masses from light to heavy shows different features, indicating possible coupling effects from target nuclei as well as projectile degrees-of-freedom [1]. In our earlier work on the ^{6}Li+^{116}Sn system [27], we have already studied the energy dependence of the potential parameters at the radius of sensitivity (R_s=9.4 fm) from optical model analysis. At this radius, all the potentials that are extracted from the elastic scattering fits for different bombarding energies have the same value [27, 43]. Similarly, some of the other elastic scattering studies of ^{6}Li from ^{27}Al, ^{28}Si, ^{90}Zr, ^{208}Pb, ^{209}Bi and ^{232}Th have also demonstrated the presence of BTA [15, 39–41]. The role of the breakup threshold value for weakly bound projectile nuclei has been previously demonstrated to be very important for the presence or absence of the "Threshold Anomaly" [1].

From the present CDCC calculations, the dynamic polarization potentials (DPP) have been extracted to study the influence of breakup coupling in the near-barrier energy regime as done in Refs. [14, 38]. From Fig. 4, in the surface region far from the radius of sensitivity [27, 43], both the real and imaginary parts vary with energy and show a repulsive and attractive nature respectively, as expected. The repulsive nature of polarization potentials is understood to lead to the so-called "BTA" [15, 39–41].

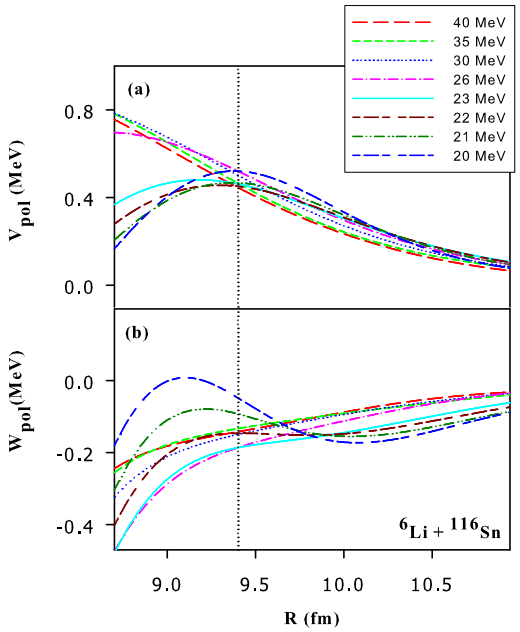

Fig. 4. (color online) Real and imaginary breakup polarization potentials generated by CDCC calculations for the ^{6}Li+^{116}Sn system. The vertical dotted line indicates the radius of sensitivity (R_s=9.4 fm) [27, 43]. For details see the text.

4 α-particle production

In the present work, we have measured the α-particle yield from the scattering of ^{6}Li by a ^{116}Sn target at below and near the Coulomb barrier energy. A separate band of α channel is clearly visible as shown in Fig. 1. Apart from the direct breakup of ^{6}Li into α+d, the measured α-particle yield may have contributions from various other possible reaction channels that includes breakup following the transfer of nucleons. Considering the Q-values for the occurrence of reactions, 1n-transfer with a Q-value of +1.28 MeV, followed by the breakup of ^{5}Li → α+p and d-pickup with a Q-value of +6.18 MeV, followed by the breakup of ^{8}Be → α+α, may be the most probable channels to be taken into consideration [23]. The α-particle production differential cross sections have been extracted following the technique mentioned by Keeley et al. [42], in which the measured α-particle yield Y_α was normalized with respect to the elastic scattering yield Y_{el} at each bombarding energy. The direct breakup-α cross sections from the present CDCC calculations were also obtained to compare with the experimentally obtained breakup-α differential cross sections at various bombarding energies. Figure 5 shows a comparison of angular distributions of

the experimental α-particle production differential cross sections and the prediction of breakup cross sections from CDCC calculations. At forward angles Coulomb breakup dominates in comparison to nuclear breakup, for all energies from above to below the barrier. This is because lower scattering angles correspond to large impact parameters, leading to Coulomb breakup being more probable at large projectile target separations. However, integrated nuclear breakup cross sections ($\sigma_{\rm bu}^{\rm nucl.}$) are found to be higher than the Coulomb breakup cross sections ($\sigma_{\rm bu}^{\rm coul.}$), as shown in Table 1. The experimental data are about one order of magnitude higher than the CDCC calculations, although the shape is quite similar.

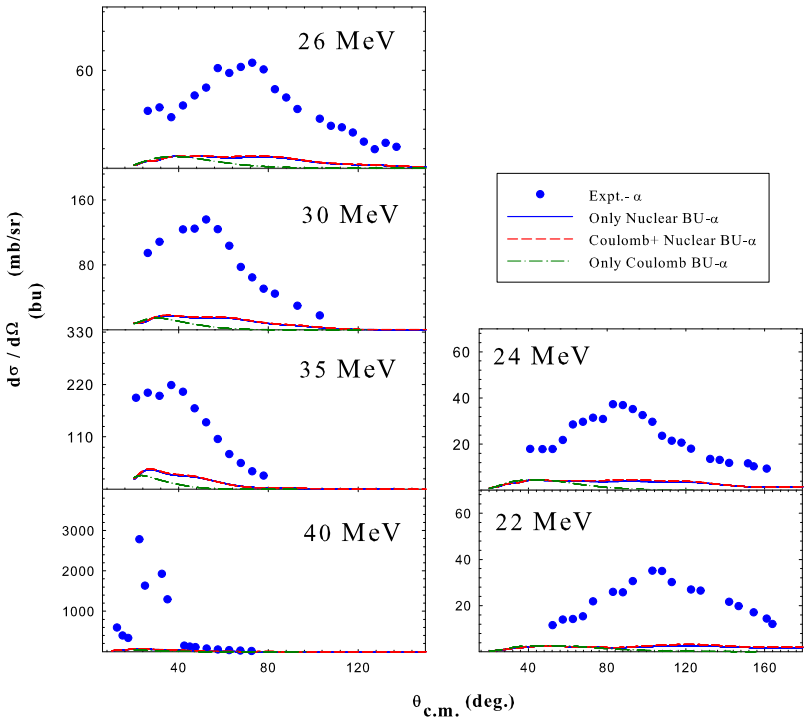

Fig. 5. (color online) α-particle differential cross section angular distributions from the scattering of ^{6}Li by a ^{116}Sn target at different projectile beam energies (circles). The results of the CDCC calculation for direct breakup of ^{6}Li into α+d with only Coulomb, only nuclear, and Coulomb+nuclear breakup couplings are shown by the dot-dashed, dashed and continuous curves respectively.

The discrepancies between the present CDCC calculations and the experimental data may be because the measured α-particle production differential cross sections account not only for the alphas coming from the breakup channel, but also from other transfer reaction mechanisms and from fusion evaporation residues. However, negligible contributions were observed from fusion evaporation residues, which have been checked using the statistical model code PACE [44]. Similar measurements for the ^{6,7}Li+^{208}Pb systems were carried out by Keeley et al., showing the large cross sections for ^{6}Li compared to ^{7}Li across the entire energy range of measurements. Also, the CDCC calculations provide a reasonable prediction of the relative α-breakup cross sections but under-predict their absolute values [42]. More recently, Jin Lei and A. M. Moro have also shown that much of the inclusive α-particle production in ^{6}Li induced reactions are due to inelastic breakup processes. The inclusive breakup cross sections have been very well reproduced with the inclusion of the contributions from inelastic breakup processes [45, 46].

5 Summary and conclusions

We have made an attempt to explore the effect of breakup coupling on elastic and α-production channels simultaneously at energies below and near the Coulomb barrier in the ^{6}Li+^{116}Sn reaction. We have obtained α-particle differential cross sections angular distributions from the scattering of ^{6}Li by a ^{116}Sn target at various energies. The measured breakup-α-particle differential cross sections and elastic scattering angular distributions have been compared with the predictions of continuum-discretized coupled channels (CDCC) calculations. The

relative importance of the nuclear, Coulomb, and total breakup have also been investigated from the predictions of CDCC calculations. Simultaneous inclusion of both nuclear and Coulomb breakup coupling can reproduce the elastic scattering angular distributions reasonably well for each bombarding energy. The effects of breakup coupling have also been studied by means of dynamic polarization potentials (DPP) as a function of radius parameter. The effects of the Coulomb breakup couplings are noticeable at forward angles, as expected, owing to the large projectile-target separation at these angles. In comparison to the Coulomb breakup couplings, nuclear breakup couplings are observed to be of paramount importance for the total direct breakup of ^{6}Li by a ^{116}Sn target. This leads to the suppression in the Coulomb-nuclear interference peak. The energy dependence of DPP is consistent with the general observation of BTA associated with the ^{6}Li projectile nuclei owing to the low breakup threshold. The results of CDCC calculations under-predict the measured α-particle differential cross sections at all energies, indicating a possible contribution from other transfer reaction mechanisms that leads to breakup-α.

The authors thank the operating staff and target laboratory staff of the TIFR-BARC Pelletron, Mumbai for their help and cooperation. Thanks are also due to Dr. R.K. Choudhury, former head, NPD, BARC for his valuable suggestions. J. Lubian and T. Correa thank CNPq and FAPERJ for partial financial support.

References

1 L. F. Canto, P. R. S. Gomes, R. Donangelo, and M. S. Hussein, Phys. Rep., **424**: 1 (2006)
2 N. Keeley, R. Raabe, N. Alamanos, and J. L. Sida, Prog. Part. Nucl. Phys., **59**: 579 (2007)
3 N. Keeley, N. Alamanos, K. W. Kemper, and K. Rusek, Prog. Part. Nucl. Sci., **63**: 396 (2009)
4 D. Patel, S. Santra, S. Mukherjee, B. K.Nayak , P. K. Rath, V. V. Parkar, and R. K. Choudhury, Pramana-J. Phys., **81**: 587 (2013)
5 B. B. Back, H. Esbensen, C. L. Jiang, and K. E. Rehm, Rev. Mod. Phys., **86**: 317 (2014)
6 L. F. Canto, P. R. S. Gomes, R. Donangelo, J. Lubian, and M. S. Hussein, Phys. Rep., **596**: 1 (2015)
7 P. R. S. Gomes, J. Lubian, L. F. Canto et al, Few-Body Syst., **57**: 165 (2016)
8 J. J. Kolata, V. Guimarães, E. F. Aguilera, Eur. Phys. J. A, **52**: 123 (2016)
9 D. Patel, S. Mukherjee, B. K. Nayak, S. V. Suryanarayana, D. C. Biswas, E. T. Mirgule, Y. K. Gupta, L. S. Danu, B. V. John, and A. Saxena, Phys. Rev. C, **89**: 064614 (2014)
10 M. S. Hussein, P. R. S. Gomes, J. Lubian, and L. C. Chamon, Phys. Rev. C, **73**: 044610 (2006)
11 S. Dubey, S. Mukherjee, D. C. Biswas et al, Phys. Rev. C, **89**: 014610 (2014)
12 S. Santra, S. Kailas, K. Ramachandran, V. V. Parkar, V. Jha, B. J. Roy, and P. Shukla, Phys. Rev. C, **83**: 034616 (2011)
13 L. F. Canto, J. Lubian, P. R. S. Gomes, and M. S. Hussein, Phys. Rev. C, **80**: 047601 (2009)
14 N. Keeley and K. Rusek, Phys. Lett. B, **427**: 1–6 (1998)
15 J. Lubian, T. Correa, B. Paes et al, Nucl. Phys. A, **791**: 24 (2007)
16 D. Patel, S. Mukherjee, D. C. Biswas, B. K. Nayak, Y. K. Gupta, L. S. Danu, S. Santra, and E. T. Mirgule, Phys. Rev. C, **91**: 054614 (2015)
17 E. F. Aguilera et al, Phys. Rev. Lett., **84**: 5058 (2000)
18 C. Signorini et al, Phys. Rev. C, **67**: 044607 (2003)
19 K. O. Pfeiffer, E. Speth, and K. Bethge, Nucl. Phys. A, **206**: 545 (1973)
20 H. Utsunomiya, S. Kubono, M. H. Tanaka, M. Sugitani, K. Morita, T. Nomura, and Y. Hamajima, Phys. Rev. C, **28**: 1975 (1983)
21 D. Patel, S. V. Suryanarayana, S. Mukherjee, B. K. Nayak, E. T. Mirgule, D. C. Biswas, A. Saxena, and J. Lubian, EPJ Web of Conf. v., **86**: 00032 (2015)
22 M. K. Pradhan, A. Mukherjee, Subinit Roy, P. Basu, A. Goswami, R. Kshetri, R. Palit, V. V. Parkar, M. Ray, M. Saha Sarkar, and S. Santra, Phys. Rev. C, **88**: 064603 (2013)
23 D. Chattopadhyay, S. Santra, A. Pal et al, Phys. Rev. C, **94**: 061602(R) (2016)
24 A. Shrivastava, A. Navin, N. Keeley, K. Mahata, K. Ramachandran, V. Nanal, V. V. Parkar, A. Chatterjee, and S. Kailas, Phys. Lett. B, **633**: 463 (2006)
25 D. H. Luong, M. Dasgupta, D. J. Hinde, R. du Rietz, R. Rafiei, C. J. Lin, M. Evers, and A. Diaz-Torres, Phys. Rev. C, **88**: 034609 (2013)
26 J. J. Kolata, Phys. Rev. C, **63**: 061604(R) (2001)
27 N. N. Deshmukh, S. Mukherjee, D. Patel et al, Phys. Rev. C, **83**: 024607 (2011)
28 M. Kamimura, M. Yahiro, Y. Iseri, Y. Sakuragi, H. Kameyama, M. Kaway, Prog. Theor. Phys. Suppl., **89**: 1 (1986)
29 N. Austern, Y. Iseri, M. Kamimura, M. Kawai, G. Rawitscher, M. Yahiro, Phys. Rep., **154**:125 (1987)
30 A. Diaz-Torres, I. J. Thompson, C. Beck, Phys. Rev. C, **68**: 044607 (2003)
31 D. R. Otomar, J. Lubian, P. R. S. Gomes et al, Phys. Rev. C **80**: 034614 (2009)
32 L. C. Chamon et al., Phys. Rev. C, **66**: 014610 (2002)
33 I. J. Thompson, Comput. Phys. Rep., **167**: 7 (1988)
34 J. Rangel, J. Lubian, L. F. Canto, and P. R. S. Gomes, Phys. Rev. C, **93**: 054610 (2016)
35 A. Di Pietro, V. Scuderi, A. M. Moro et al, Phys. Rev. C, **85**: 054607 (2012)
36 N. Keeley, N. Alamanos, K. W. Kemper, and K. Rusek, Phys. Rev. C, **82**: 034606 (2010)
37 D. R. Otomar, P. R. S. Gomes, J. Lubian, L. F. Canto, and M. S. Hussein, Phys. Rev. C, **87**: 014615 (2013)
38 I. J. Thompson et al, Nucl. Phys. A, **505**: 84 (1989)
39 H. Kumawat, V. Jha, B. J. Roy, V. V. Parkar, S. Santra, V. Kumar, D. Dutta, P. Shukla, L. M. Pant, A. K. Mohanty, R. K. Choudhury, and S. Kailas Phys. Rev. C, **78**: 044617 (2008)
40 S. Santra, V. V. Parkar, K. Ramachandran, U. K. Pal, A. Shrivastava, B. J. Roy, B. K. Nayak, A. Chatterjee, R. K. Choudhury, S. Kailas, Phys. Lett. B, **677**: 139–144 (2009)
41 Shradha Dubey, S. Mukherjee, D. C. Biswas et al, Phys. Rev. C, **89**: 014610 (2014)
42 G. R. Kelly, N. J. Davis, R. P. Ward et al, Phys. Rev. C, **63**: 024601 (2000)
43 G. R. Satchler, Phys. Rep., **199**: 147 (1991)
44 A. Gavron, Phys. Rev. C, **21**: 230 (1980)
45 Jin Lei and A. M. Moro, Phys. Rev. C, **95**: 044605 (2017)
46 Jin Lei and A. M. Moro, Phys. Rev. C, **92**: 044616 (2015)